AGU PUBLICATIONS

Geophysical Research Letters

RESEARCH LETTER
10.1002/2015GL063751

**Key Points:**
- The article presents numerical modeling of anomalous absorption
- A scaling law is derived for different plasma parameters
- The numerically obtained scaling law is consistent with experiments

**Correspondence to:**
B. Eliasson,
bengt.eliasson@strath.ac.uk

**Citation:**
Eliasson, B., and K. Papadopoulos (2015), Numerical study of anomalous absorption of O mode waves on magnetic field-aligned striations, *Geophys. Res. Lett.*, *42*, doi:10.1002/2015GL063751.

Received 6 MAR 2015
Accepted 28 MAR 2015
Accepted article online 1 APR 2015



# Numerical study of anomalous absorption of O mode waves on magnetic field-aligned striations

**B. Eliasson[1,2] and K. Papadopoulos[2]**

[1]SUPA Physics Department, University of Strathclyde, Glasgow, UK, [2]Departments of Physics and Astronomy, University of Maryland, College Park, Maryland, USA

**Abstract** Simple expressions that describe mode conversion and anomalous absorption of ordinary (O) mode waves injected at angles between the vertical and magnetic zenith to upper hybrid (UH) oscillations in the presence of field-aligned density striations are presented. The absorption takes place in a region above the UH resonance layer where the striations allow trapped eigenmodes, leading to excitation of large-amplitude UH waves. The derivation of the expressions is guided by dimensional analysis and numerical simulations. The results are relevant in interpreting high-latitude heating experiments where anomalous absorption due to striations plays a crucial role.

## 1. Introduction

The interaction of HF radio waves with the ionospheric plasma in the vicinity of the upper hybrid (UH) resonance layer plays a critical role in the physics of ionospheric modifications and artificial ionospheric turbulence. It is believed that the UH interaction region gives rise to features such as the downshifted maximum and continuum in the stimulated electromagnetic emissions [*Mjølhus*, 1998; *Leyser*, 2001]. Early experiments at Platteville [*Cohen and Whitehead*, 1970], Tromsø [*Stubbe et al.*, 1982; *Jones et al.*, 1984; *Stocker et al.*, 1993], and in Russia [*Getmantsev et al.*, 1973] showed a drastic increase of absorption of the ordinary (O) mode pump and test waves after a few seconds if the wave frequencies were below the maximum UH frequency of the ionosphere. It has been observed that when the electromagnetic beam is directed along the magnetic zenith (MZ), parallel to the magnetic field lines [*Gurevich et al.*, 2002], or between the MZ and the Spitze angle [*Rietveld et al.*, 2003; *Honary et al.*, 2011], there is an increase of the electron temperature in the heated region. The observations are consistent with the formation of small-scale magnetic field-aligned striations, followed by mode conversion of the O mode pump and test waves to UH waves trapped in the striations [*Graham and Fejer*, 1976; *Vas'kov and Gurevich*, 1976; *Dysthe et al.*, 1982; *Jones et al.*, 1984; *Mjølhus*, 1985; *Gurevich et al.*, 1995, 1996]. The UH oscillations are then responsible for heating the electrons and increasing further the amplitude of the striations [*Lee and Fejer*, 1978; *Dysthe et al.*, 1982; *Inhester*, 1982; *Gurevich et al.*, 1995]. Striations measured in situ by a sounding rocket flown through the heater beam at Arecibo [*Kelley et al.*, 1995] had a typical width of 7 m, a mean depletion depth of about 6%, and a separation of about 15 m.

The aim of this paper is to numerically study the efficiency of mode conversion of an O mode to UH waves on field-aligned striations and its dependence on ionospheric plasma parameters. The study concentrates on cases where the resonant UH interaction and absorption processes take place in a separate region below the turning point of the O mode wave. The results have implications on the electron heating at the UH layer and on the fraction of the electromagnetic wave energy that reaches the critical layer of the O mode where it can excite Langmuir turbulence.

## 2. Optimal Angle of Incidence

An important parameter is the angle of incidence $\chi = \chi_{UH}$ to the vertical line in the plane of the magnetic field (cf. equation (6) below) that results in O mode propagation parallel to the magnetic field lines at the UH layer. In this case the wave electric field is directed across the striations and the O mode is most efficiently converted to UH waves trapped in the striations [cf. *Mjølhus*, 1985, Figure 5]. To calculate the optimal angle of incidence $\chi_{UH}$, we assume that the ionospheric profile is vertically stratified, and that the geomagnetic field is directed at an angle $\theta$ to the vertical line. When the O mode propagates through the

ionosphere, its frequency $\omega$ and horizontal wave vector component $k_x$ are conserved. Since the wave is injected from a ground-based transmitter in free space, we have

$$k_x = \frac{\omega}{c}\sin\chi\ . \tag{1}$$

At the altitude where the wave propagates parallel to the magnetic field, we also have

$$k_x = k\sin\theta, \tag{2}$$

where $k = \sqrt{k_x^2 + k_z^2}$ is the local magnitude of the wave vector. At this altitude, the O mode propagates as a left-hand polarized (L) mode wave, obeying the dispersion relation

$$\frac{c^2k^2}{\omega^2} = 1 - \frac{\omega_{pe}^2}{\omega(\omega+\omega_{ce})}\ , \tag{3}$$

where $\omega_{pe} = \sqrt{n_0e^2/(\epsilon_0 m_e)}$ is the electron plasma frequency and $\omega_{ce} = eB_0/m_e$ the electron cyclotron frequency. Here $n_0$ is the local electron number density, $e$ is the magnitude of the electron charge, $m_e$ is the electron mass, and $\epsilon_0$ is the electric permittivity in vacuum. Eliminating $k$ and $k_x$ from equations (1)–(3) gives

$$\frac{\sin^2\chi}{\sin^2\theta} = 1 - \frac{\omega_{pe}^2}{\omega(\omega+\omega_{ce})}\ . \tag{4}$$

For example, using $\omega = \omega_{pe}$ and eliminating $\omega_{pe}$ in equation (4), we find the Spitze angle

$$\chi = \chi_S = \arcsin\left(\sqrt{\frac{Y}{1+Y}}\sin\theta\right)\ , \tag{5}$$

where the O mode is efficiently converted to a Z mode wave as it reaches the critical layer [e.g., *Mjølhus*, 1990]. In equation (5) $Y = \omega_{ce}/\omega$. Using instead $\omega = \omega_{UH} = \sqrt{\omega_{pe}^2 + \omega_{ce}^2}$ and eliminating $\omega_{pe}$ in equation (4) gives the optimal incidence angle

$$\chi = \chi_{UH} = \arcsin\left(\sqrt{Y}\sin\theta\right) \tag{6}$$

that results in O mode propagation parallel to the magnetic field when it reaches the UH layer. For typical parameters at High Frequency Active Auroral Research Program (HAARP), $\theta = 14.5°$, $\omega_{ce} = 9.09 \times 10^6 s^{-1}$, and $\omega = 20.1 \times 10^6 s^{-1}$ we find $\chi_S = 8.0°$ and $\chi_{UH} = 9.6°$. Hence, $\chi_{UH}$ is between the Spitze and MZ. This is consistent with the maximum electron heating observed at an incidence angle between the Spitze and MZ [e.g., *Honary et al.*, 2011].

## 3. Simulation Setup

We next consider a two-dimensional simulation geometry in the *x*-*z* plane with the magnetic field directed along the negative *z* axis. For the auroral zone geometry, where the geomagnetic field is directed almost vertically downward, O mode propagation along the *z* axis is justified up to a few wavelengths away from the critical layer of the O mode. The ambient ionospheric (ion and electron) number density profile is taken as $n_0(z) = n_{0,max}\exp\left[-(z-z_{max})^2/L_{n0}^2\right]$, where $n_{0,max}$ is the number density at the $F_2$ peak located at the altitude $z = z_{max}$, and $L_{n0}$ is the ionospheric length scale. The total plasma density, including a striation superimposed on the ambient density at $x = 0$, is taken as $n(x,z) = n_0(z)\left[1 - \delta\tilde{n}_{str}\exp\left(-x^2/D_{str}^2\right)\right]$, where $\delta\tilde{n}_{str}$ is the relative density depletion and $D_{str}$ is the transverse size of the striation. Figure 1 shows a density striation with $D_{str} = 2$ m, $\delta\tilde{n}_{str} = 0.1$, $n_{0,max} = 1.436 \times 10^{11}$ $m^{-3}$ (corresponding to the peak plasma frequency $f_{oF_2} = 3.40$ MHz), $z_{max} = 242$ km, and $L_{n0} = 31.62$ km. For periodic boundary conditions along the *x* direction, Figure 1 represents a grid of striations separated by the transverse simulation box size $L_x = 12$ m. The used pump frequency $\omega = 20.1 \times 10^6$ $s^{-1}$ ($f_0 = 3.20$ MHz) corresponds to a vacuum wavelength $\lambda_0 = c/f_0 = 93.75$ m. For the chosen parameters, the critical altitude where the pump frequency equals the ambient plasma frequency is at $z_O = 230.96$ km (the dotted line in Figure 1). The ambient magnetic field $B_0 = 5.17 \times 10^{-5}$ T corresponds to electron cyclotron frequency $\omega_{ce} = 9.09 \times 10^6$ $s^{-1}$ (1.45 MHz). The UH resonance where the pump frequency equals the UH frequency in the unperturbed ionosphere is at $z_{UH} = 223.27$ km (the dashed line in Figure 1). The critical surface $\omega = \omega_{UH}$ is

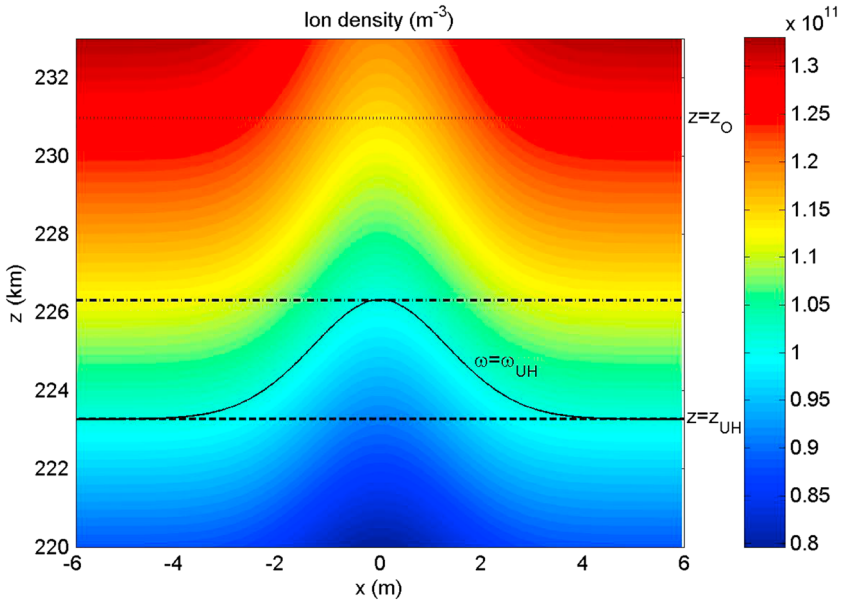


**Figure 1.** Spatial profile of the total ion density. A striation of size $D_{str} = 2$ m and relative density depletion $\delta\tilde{n}_{str} = 0.1$ is centered at $x = 0$. The dashed line indicates the altitude $z = z_{UH} = 223.27$ km of the bottom of the UH layer where $\omega = \omega_{UH}$ outside the striation. The altitude where $\omega = \omega_{UH}$ is indicated with a solid line, while the dash-dotted line marks the limiting altitude $z = 226.29$ km of the top of the UH layer, where, locally, $\omega = \omega_{UH}$ at the center of the striation. The UH interaction region is constrained between the two altitudes. The critical altitude $z = z_O$ of the O mode wave is indicated with a dotted line.

indicated with a solid line in Figure 1, where $\omega_{UH}(x,z) = \sqrt{\omega_{pe}^2(x,z) + \omega_{ce}^2}$ is the UH resonance frequency and $\omega_{pe}(x,z) = \sqrt{n(x,z)e^2/(\epsilon_0 m_e)}$ is the local electron plasma frequency. In Figure 1 the upper boundary of the UH interaction layer is indicated with a dash-dotted line. Notice that the O mode will propagate up to or near the critical altitude for angles smaller than or close to the Spitze angle.

In order to have well-defined, transmitted, and absorbed waves through the UH region this paper focuses on cases where the UH interaction region is below the critical altitude of the O mode, i.e., the dotted line should be at a higher altitude than the dash-dotted line in Figure 1. The separation between the altitudes of the critical and UH layers is approximately $z_O - z_{UH} \approx Y^2 L_{UH}$, where the local length scale is $L_{UH} = 1/|\mathrm{d}\ \ln(n_0)/\mathrm{d}z|$ at $z = z_{UH}$, and the separation between the bottom and top of the UH interaction region is $\Delta z_{UH} \approx \delta\tilde{n}_{str} L_{UH}$. Hence, the condition for the separation of the UH interaction region from the O mode critical layer is

$$Y^2 > \delta\tilde{n}_{str}. \tag{7}$$

For example, for a relative striation density depletion of $\delta\tilde{n}_{str} = 0.1$, the condition is fulfilled for $Y > 0.32$. For the typical electron cyclotron frequency of 1.45 MHz at HAARP and relative striation depth $\delta\tilde{n}_{str} = 0.1$, the UH interaction region is separated from the O mode critical layer only for transmission frequencies below 4.5 MHz If $Y^2 < \delta\tilde{n}_{str}$, the critical altitude of the O mode wave will be located within the UH interaction region, making the interpretation of the absorption process more complicated.

On the fast UH and O mode timescale, we assume that the ions are immobile and contribute only to a neutralizing background of the plasma. For the high-frequency electron dynamics and the electromagnetic field, we solve the dynamical equations for the slowly varying complex envelopes, with the substitution $\partial/\partial t \to \partial/\partial t - i\omega$. There is a clear separation of length scales in the problem, where the electromagnetic waves have wavelengths of the order 100 m, while the UH waves have typical wavelengths of less than a meter. This poses a computational problem since the numerical scheme must resolve both length scales, while the time step is limited by the Courant condition to the smallest grid size, which in our case is in the $x$ direction. To resolve this problem, we follow the techniques presented in

*Eliasson* [2013] and separate the electric field into an electrostatic, curl-free part $\mathbf{E}_{ES} = -\nabla\phi$, where the scalar potential is obtained from Poisson's equation

$$\nabla^2\phi = \frac{e}{\epsilon_0} n_e \tag{8}$$

and an electromagnetic, divergence-free part $\mathbf{E}_{EM}$ defined by

$$\frac{\partial \mathbf{A}}{\partial t} = i\omega\mathbf{A} - \mathbf{E}_{EM} \tag{9}$$

where $\mathbf{A}$ is the vector potential defined by its relation to the magnetic field $\mathbf{B} = \nabla\times\mathbf{A}$ and the Coulomb gauge $\nabla\cdot\mathbf{A} = 0$. The electromagnetic electric field is obtained from

$$\frac{\partial \mathbf{E}_{EM}}{\partial t} = i\omega\mathbf{E}_{EM} - \frac{e}{\epsilon_0}\nabla^{-2}\nabla\times[\nabla\times(\overline{n\mathbf{v}_e})] \,. \tag{10}$$

The overbar denotes spatial averaging in the $x$ direction, so that the electric current and the electromagnetic fields $\mathbf{E}_{EM}$ and $\mathbf{A}$ depend only on the vertical coordinate $z$ and on time, but not on the transverse coordinate $x$. This allows us to take about 50–100 times longer time steps, since the Courant condition now limits the time step by $\Delta t \lesssim \Delta z/c$ instead of the much more restrictive $\Delta t \lesssim \Delta x/c$.

The electron dynamics is governed by the continuity and momentum equations, respectively,

$$\frac{\partial n_e}{\partial t} = i\omega n_e - \nabla\cdot(n\mathbf{v}_e) \tag{11}$$

and

$$\frac{\partial \mathbf{v}_e}{\partial t} = i\omega\mathbf{v}_e - \frac{e}{m_e}(\mathbf{E} + \mathbf{E}_{ext} + \mathbf{v}_e\times\mathbf{B}_0) - \frac{3v_{Te}^2}{n}\kappa\nabla n_e \,, \tag{12}$$

where $\mathbf{E} = \mathbf{E}_{ES} + \mathbf{E}_{EM}$ is the total electric field, $\mathbf{B}_0 = B_0\hat{z}$ is the downward directed magnetic field, $v_{Te} = \sqrt{k_B T_e/m_e}$ is the electron thermal speed, $T_e$ is the electron temperature, $k_B$ is Boltzmann's constant, and $\kappa = 1/(1-4Y^2)$ accounts for a kinetic dispersive effect for UH branch of the electron Bernstein waves that becomes important for low pump frequencies within a few electron cyclotron harmonics [e.g., *Lominadze*, 1981]. A pseudo-spectral method is used to calculate the spatial derivatives accurately, with typical grid sizes $\Delta x = 4$ cm in the transverse direction and $\Delta z = 17$ m in the longitudinal direction, and a standard fourth-order Runge-Kutta scheme is used to advance the solution in time, with a time step of $\Delta t = 10^{-8}$ s. The size of the simulation box is 13 km in the $z$ direction, and different widths are used in the $x$ direction to match the widths of the striations. To resonantly drive an upward propagating (opposite to the direction of $\mathbf{B}_0$) L mode wave below the UH interaction region, a right-hand circularly polarized external field $\mathbf{E}_{ext} = (\hat{\boldsymbol{x}} + i\hat{\boldsymbol{y}})\ \exp(ik)\exp\left[-(z-z_0)^2/D_{ext}^2\right]$ is used, centered at $z_0$ near the bottom of the simulation box and with a vertical width $D_{ext} = 250$ m. The wave number $k$, given by equation (3), matches that of the propagating L mode wave. A damping layer for the electromagnetic wave is introduced near the top of the simulation box to absorb O mode waves that have propagated through the UH interaction region. The external field is switched on at the start of the simulation $t = 0$.

## 4. Numerical Results

Key physics characteristics of the O to UH mode conversion are illustrated in Figures 2–4 at time $t = 0.1$ ms into the simulations. The O mode wave injected from the bottom side is continuously converted to UH waves, and the UH wave amplitude gradually increases with time. The fraction of O mode wave energy converted to UH waves quickly reaches a steady state, and for times larger than 0.1 ms, the amplitude profiles of the electromagnetic wave undergo only very slight changes. To study the absorption of the O mode wave, it is therefore sufficient to run the simulations up to $t = 0.1$ ms and then record the results.

Figure 2 shows examples of simulations using the electron temperature $T_e = 4000$ K and three different striations with transverse sizes $D_{str} = 1$ m, $D_{str} = 2$ m, and $D_{str} = 4$ m. In order to keep the packing factor $\eta = 2D_{str}/L_x$ unchanged, the simulations were performed with a box size in the $x$ direction of 6 m, 12 m, and 24 m, respectively. Note the following: (i) The wave energy is efficiently mode converted at quantized

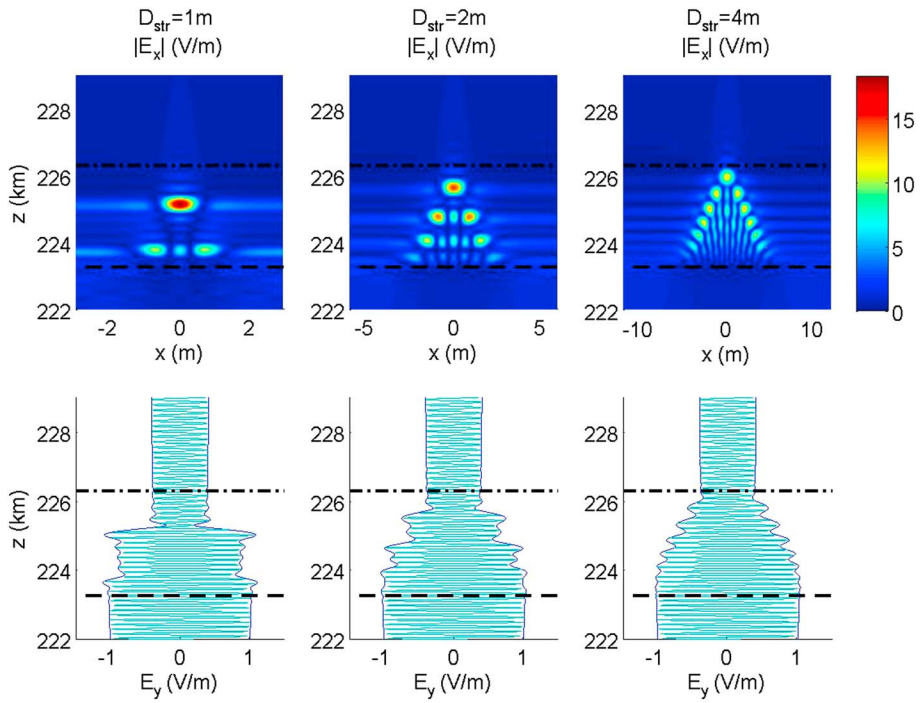


**Figure 2.** (top) The $x$ component of the electric field showing trapped UH waves and (bottom) the $y$ component of the electric field representing the O mode electromagnetic wave, for density striations with the widths $D_{str} = 1$ m, 2 m, and 3 m, relative striation depth $\delta\tilde{n}_{str} = 0.1$, and electron temperature $T_e = 4000$ K. The simulation domain is adjusted to keep the packing factor $\eta = 2D_{str}/L_x = 0.333$ the same for the three cases. The dashed line indicates the altitude $z = 223.27$ km of the UH layer where $\omega = \omega_{UH}$ and the dash-dotted line the altitude $z = 226.29$ km where locally $\omega = \omega_{UH}$ at the center of the striation.

heights where the wave frequency is equal to quantized eigenfrequencies of trapped UH waves, as discussed by *Mjølhus* [1998]. (ii) The absorption layer $\Delta z_{UH}$ starts at the altitude where $\omega = \omega_{UH}$ outside the striation, but its extent is bracketed by the altitude where locally $\omega = \omega_{UH}$ at the center of the striation. (iii) As the striation width increases, the absorption width increases occupying a larger fraction of $\Delta z_{UH}$, the number of layers where the UH waves are resonantly absorbed increases, and the resonant layers move closer to each other. The total number of UH resonances (both odd and even) in a striation is roughly given by [*Mjølhus*, 1998]

$$M = \frac{1}{\pi}\int \sqrt{\frac{\delta n}{n_0}}\frac{\mathrm{d}x}{\lambda_{De}\sqrt{3\kappa}}\ , \tag{13}$$

but due to symmetry, only even ($M$/2) resonances are excited. Here $\lambda_{De} = v_{Te}/\omega_{pe}$ is the electron Debye length. In our case we have $\delta n/n_0 = \delta\tilde{n}_{str}\exp\left(-x^2/D_{str}^2\right)$, and the integral can be evaluated as

$$M = \sqrt{\frac{2\delta\tilde{n}_{str}}{3\pi\kappa}}\frac{D_{str}}{\lambda_{De}}\ . \tag{14}$$

For the parameters used in Figure 2, we have $\lambda_{De} \approx 0.014$ m, $\delta\tilde{n}_{str} = 0.1$, and $\kappa = 5.5$. For the cases $D_{str} = 1$ m, 2 m, and 4 m, the number of even resonances are $M/2 \approx 2.3$, 4.5, and 9, respectively, which is consistent with Figure 2, where respectively 2, 4, and 8 resonances are visible. (iv) Most importantly, in all three cases, the relative absorption, as seen by the value of $E_y$ at Figure 2 (bottom) remains the same. The $y$ component of the electric field decreases about 50% in amplitude above the UH layer, implying that about 75% of the wave energy is absorbed and converted to UH waves.

When instead changing the electron temperature (cf. Figure 3), the wavelength of the UH wave (Figure 3, top) increases with increasing temperature; for lower temperatures the number of resonant layers increases and the resonant layers move closer to each other. Similar to Figure 2, the absorption layer is constrained to $\Delta z_{UH}$ starting where $\omega = \omega_{UH}$ outside the striation up to an altitude below where, locally, $\omega = \omega_{UH}$ at the center of the striation. Most importantly, the relative absorption remains the same for different temperatures, as seen by the value of $E_y$ at Figure 3 (bottom).

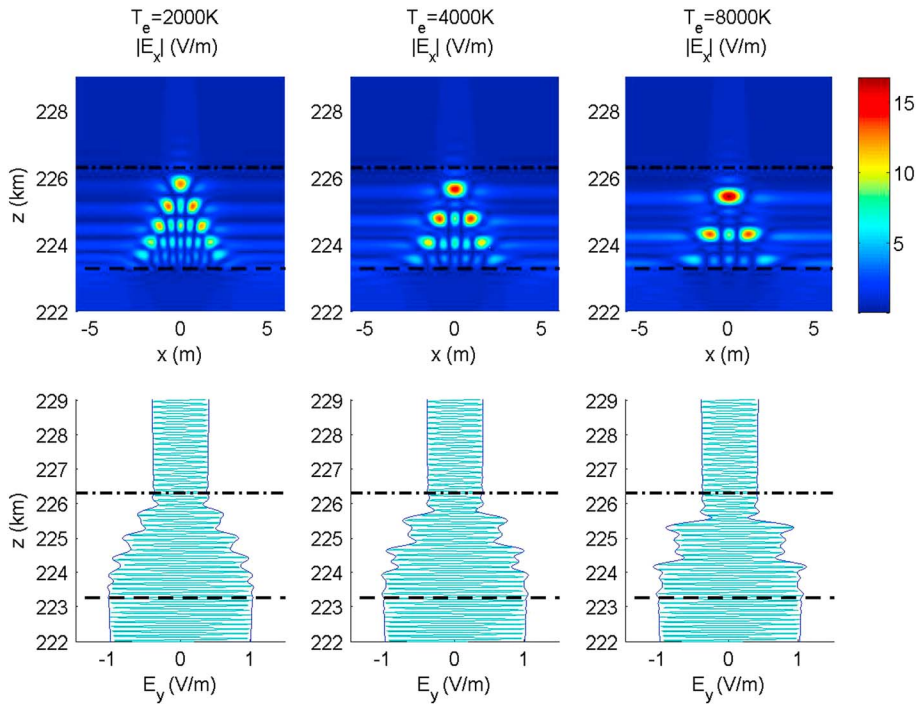


**Figure 3.** The same as in Figure 2 for electron temperatures $T_e = 2000$ K, 4000 K, and 8000 K, using density striation with the width $D_{str} = 2$ m and relative striation density depletion $\delta\tilde{n}_{str} = 0.1$.

In contrast, we see in Figure 4 that an increase of $\delta\tilde{n}_{str}$ from 0.05 to 0.15 leads to a reduction of the O mode amplitude above the UH interaction region by almost an order of magnitude. Hence, the striation depth is a crucial parameter for the anomalous absorption of the O mode wave. For deeper striations, the interaction region $\Delta z_{UH}$ increases, leading to a larger number of resonant layers, while the distance between the layers depend only weakly on $\delta\tilde{n}_{str}$.

## 5. Scaling Analysis

From Figures 2 and 3, we conclude that the absorption of O mode waves to UH waves on striations does not significantly depend on $D_{str}$ and $T_e$ while keeping other parameters constant. By dimensional analysis of the governing equations, one finds that the physics of the system depends only on four local dimensionless parameters: $\eta$, $\delta\tilde{n}_{str}$, $\Delta z_{UH}/\lambda_0$. ($\Delta z_{UH}$ is the vertical width of the UH interaction region, between the dash-dotted and dashed lines in Figure 1), and $Y = \omega_{ce}/\omega_0$. Note that $\Delta z_{UH}$ also depends on $D_{str}$, $Y$, and parameters defining the ionospheric profile. By performing a set of simulations similar to the ones in Figures 2–4 for different combinations of the parameters, we have found a simple expression for the transmission coefficient (transmitted intensity above the striation divided by incident intensity below the striation)

$$T \approx \frac{|E_{yT}|^2}{|E_{yT0}|^2} = \exp\left[-3.24\,\delta\tilde{n}_{str}\frac{\Delta z_{UH}}{\lambda_0}\left(\eta - 1.4\eta^2\right)\left(\frac{1}{Y} - 1.09\right)\right], \tag{15}$$

estimated as the squared amplitude ratio of the transmitted electric field above the UH interaction region $E_{yT}$ and $E_{yT0}$ with and without striation, respectively. The formula is valid for typical ionospheric parameters $0.2 < Y < 0.46$, $\eta < 0.5$, and $\delta\tilde{n}_{str} \lesssim Y^2$ (cf. equation (7)).

A comparison between numerically obtained values of the transmission coefficient and the expression (15) is shown in Figure 5, with good agreement. As seen in Figure 5a, the transmission coefficient in general decreases with increasing packing factor $\eta$, since there are more striations per given area to absorb wave energy. However, for large values $\eta > 0.25$, the absorption becomes less efficient and the curves in Figure 5a have a minimum at $\eta \approx 0.35$. This is reflected in the term proportional to $\eta^2$ in the exponential in

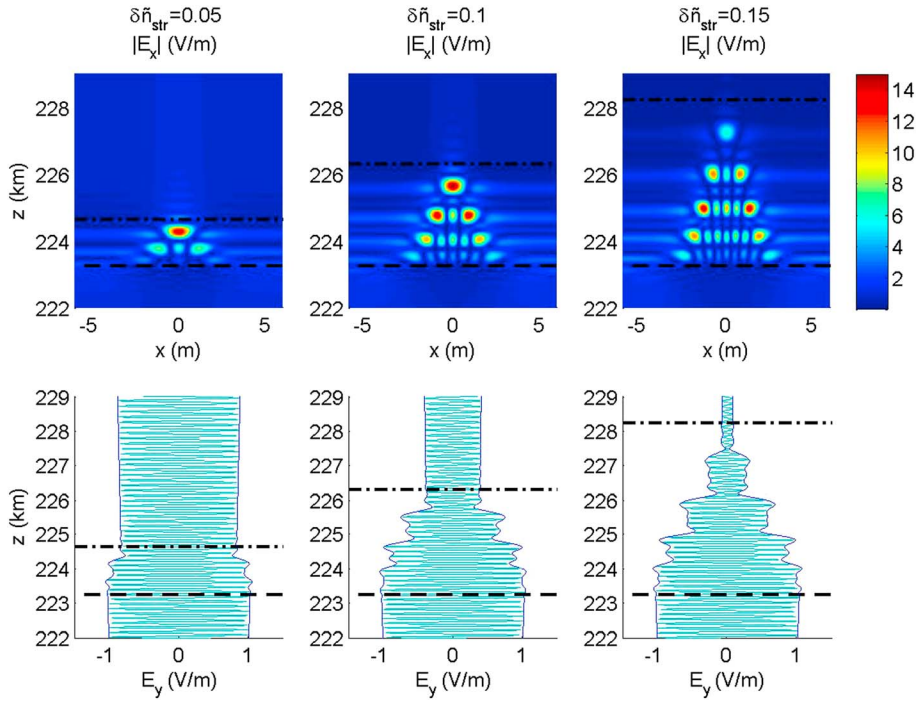


**Figure 4.** The same as Figure 2 for relative striation depths $\delta\tilde{n}_{str} = 0.05$, 0.1, and 0.15, width $D_{str} = 2$ m, and electron temperature $T_e = 4000$ K.

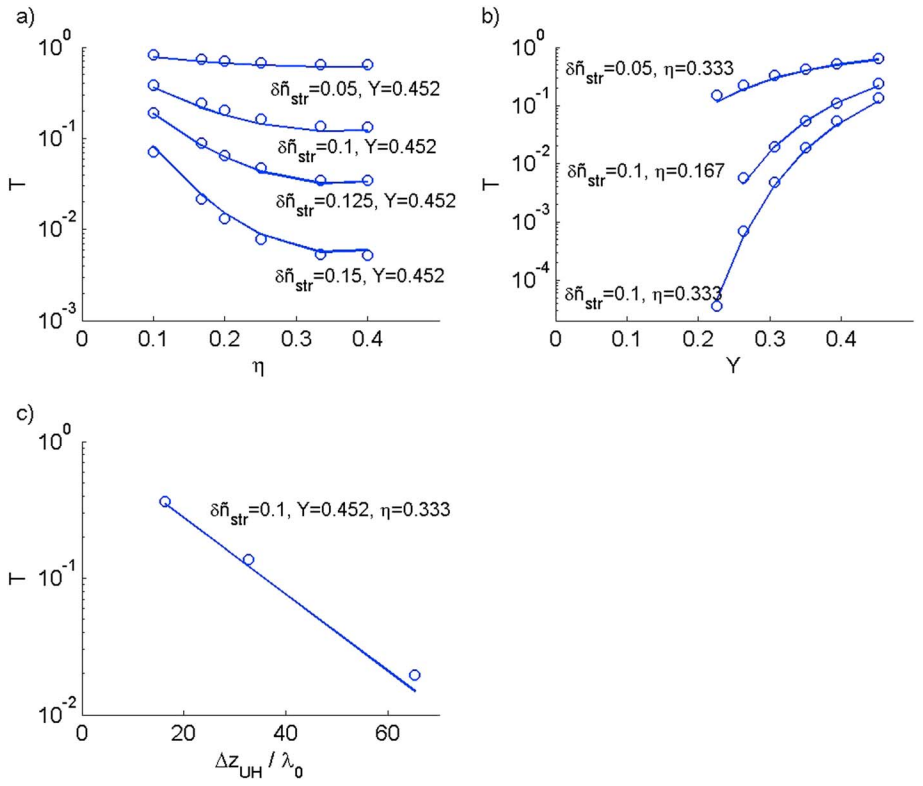


**Figure 5.** Transmission coefficients for different parameters. The circles show numerically obtained transmission coefficients via full wave simulations, while the solid lines indicate values obtained from expression (15).

equation (15) and is due to close-packing effects which changes the average dielectric properties of the plasma and reduces the effectiveness of absorption for densely packed striations. On the other hand, we see in Figures 4, 5a, and 5b that an increase of $\delta\tilde{n}_{str}$ from 0.05 to 0.1–0.15 can decrease the transmitted electric field by more than a factor 10 and the corresponding transmission coefficient by a few orders of magnitude. An increase of $\delta\tilde{n}_{str}$ increases both the depth of the striation locally and the vertical width of the UH interaction region (cf. Figure 4). To first order, $\Delta z_{UH} \approx \delta\tilde{n}_{str} L_{UH}$, and hence, the expression in the exponential of (15) is approximately proportional to $\delta\tilde{n}_{str}^2$. Therefore, most of the injected wave energy will be absorbed when the striations have grown to a significant amplitude. Finally, the results in Figure 5c, indicating a decrease of $T$ with $\Delta z_{UH}$, were obtained by keeping $\delta\tilde{n}_{str}$, $Y$, and $\eta$ constant, while halving and doubling the ionospheric vertical length scale $L_{n0}$, so as to decrease and increase $\Delta z_{UH}$ proportionally.

The numerical results are in qualitative agreement with the theoretical expression for the transmission coefficient for small amplitude striations, corresponding to $\delta\tilde{n}_{str} L_{UH}/D_{str} \ll 1$, given in equation (2a) of *Mjølhus* [1985], which for parallel propagation of the O mode along the striations can be written as

$$T = \exp\left[-\pi^2 \frac{L_{UH}}{\lambda_0} \frac{(1-Y)^2}{\sqrt{Y}} \left\langle \left(\frac{\delta n}{n_0}\right)^2 \right\rangle\right], \tag{16}$$

where the angle brackets denote spatial averaging and $\delta n$ is the density perturbation due to the striations. In our case, $\delta n/n_0 = -\delta\tilde{n}_{str}\exp\left(-x^2/D_{str}^2\right) + \delta\tilde{n}_{str}(\eta/2)\sqrt{\pi}$, where we have subtracted the mean density and a spatial average over the simulation box gives $\left\langle (\delta n/n_0)^2 \right\rangle \approx \sqrt{\pi/2}\left(\delta\tilde{n}_{str}^2/2\right)\left(\eta - \sqrt{\pi/2}\,\eta^2\right)$, which also recovers the close-packing effect governed by the $\eta^2$ term in equation (15); the coefficient $\sqrt{\pi/2} \approx 1.25$ in front of $\eta^2$ is comparable to the coefficient 1.4 obtained numerically in equation (15). The decrease of the transmission coefficient for the relative decrease of the magnetic field $Y$ seen in Figure 5b is also consistent with equation (16). In general, $T + A + R = 1$, where $A$ and $R$ are the absorption and reflection coefficients, respectively [e.g., *Mjølhus*, 1985]. *Mjølhus* [1985] also predicted a significant reflection of O mode waves by the UH layer for wave propagating into denser plasma, which would limit the absorption coefficient to $A < 0.5$. A reflection by the UH interaction region would give rise to a standing wave pattern below the UH layer, which, however, is not seen in Figures 2–4. Hence, the numerical results indicate that $R \approx 0$ and $A = 1 - T$. The numerical results are consistent with experiment [e.g., *Cohen and Whitehead*, 1970; *Stubbe et al.*, 1982], where the amplitude of reflected O mode waves on the ground drops about 10–15 dB after the striations have had time to develop. If there is no direct reflection by the UH layer, the O mode must travel through the UH layer twice: first, as an upgoing wave into denser plasma to the turning point of the O mode, and then as a downgoing wave propagating out from the plasma. If the transmission coefficient is the same for upgoing and downgoing waves, the total transmission coefficient is $T_{tot} \approx T^2$ where $T$ is given by equation (15). As is evident from Figure 5, an injected wave could then be absorbed and decreased in power several tens of decibels before returning back to ground.

**Acknowledgments**

This work was supported by the MURI grant FA95501410019. B.E. acknowledges support from the EPSRC (UK), grant EP/M009386/1. Simulation data supporting the figures can be requested from Bengt Eliasson, e-mail: bengt.eliasson@strath.ac.uk.

The Editor thanks Thomas Leyser and an anonymous reviewer for their assistance in evaluating this manuscript.

## References

Cohen, R., and J. D. Whitehead (1970), Radio-reflectivity detection of artificial modification of the ionospheric *F* layer, *J. Geophys. Res.*, *75*(31), 6439–6445, doi:10.1029/JA075i031p06439.

Dysthe, K. B., E. Mjølhus, H. L. Pécseli, and K. Rypdal (1982), Thermal cavitons, *Phys. Scr.*, *T2/2*, 548–559.

Eliasson, B. (2013), Full-scale simulations of ionospheric Langmuir turbulence, *Mod. Phys. Lett. B*, *27*(8), 1330005.

Getmantsev, G. G., G. P. Komrakov, Y. S. Korobkov, L. F. Mironenko, N. A. Mityakov, V. O. Rapoport, V. Y. Trakhtengerts, V. L. Frolov, and V. A. Cherepovitskii (1973), Some results of investigations of nonlinear phenomena in the F-layer of the ionosphere, *JETP Lett.*, *18*, 364.

Graham, K. N., and J. A. Fejer (1976), Anomalous radio wave absorption due to ionospheric heating effects, *Radio Sci.*, *11*(12), 1057–1063, doi:10.1029/RS011i012p01057.

Gurevich, A. V., A. V. Lukyanov, and K. P. Zybin (1995), Stationary striations developed in the ionospheric modification, *Phys. Rev. Lett.*, *75*, 2622–2625.

Gurevich, A. V., A. V. Lukyanov, and K. P. Zybin (1996), Anomalous absorption of powerful radio waves on the striations developed during ionospheric modification, *Phys. Lett. A*, *211*, 363–372, doi:10.1016/0375-9601(95)00970-1.

Gurevich, A. V., K. P. Zybin, H. C. Carlson, and T. Pedersen (2002), Magnetic zenith effect in ionospheric modifications, *Phys. Lett. A*, *305*, 264–274.

Honary, F., N. Borisov, M. Beharrell, and A. Senior (2011), Temporal development of the magnetic zenith effect, *J. Geophys. Res.*, *116*, A06309, doi:10.1029/2010JA016029.

Inhester, B. (1982), Thermal modulation of the plasma density in ionospheric heating experiments, *J. Atmos. Terr. Phys.*, *44*(12), 1049–1059.

Jones, T. B., T. Robinson, P. Stubbe, and H. Kopka (1984), Frequency dependence of anomalous absorption caused by high power radio waves, *J. Atmos. Terr. Phys.*, *46*(2), 147–153, doi:10.1016/0021-9169(84)90140-5.

Kelley, M. C., T. L. Arce, J. Salowey, M. Sulzer, W. T. Armstrong, M. Carter, and L. Duncan (1995), Density depletions at the 10-m scale induced by the Arecibo heater, *J. Geophys. Res.*, *100*(A9), 17,367–17,376, doi:10.1029/95JA00063.

Lee, M.-C., and J. A. Fejer (1978), Theory of short-scale field-aligned density striations due to ionospheric heating, *Radio Sci.*, *13*(5), 893–899, doi:10.1029/RS013i005p00893.

Leyser, T. B. (2001), Stimulated electromagnetic emissions by high-frequency electromagnetic pumping of the ionospheric plasma, *Space Sci. Rev.*, *98*, 223–328.

Lominadze, D. G. (1981), *Cyclotron Waves in Plasmas*, Pergamon Press, New York.

Mjølhus, E. (1985), Anomalous absorption and reflection in ionospheric radio modification experiments, *J. Geophys. Res.*, *90*(A5), 4269–4279, doi:10.1029/JA090iA05p04269.

Mjølhus, E. (1990), On linear mode conversion in a magnetized plasma, *Radio Sci.*, *25*(6), 1321–1339, doi:10.1029/RS025i006p01321.

Mjølhus, E. (1998), Theoretical model for long time stimulated electromagnetic emission generation in ionospheric radio modification experiments, *J. Geophys. Res.*, *103*(A7), 14,711–14,729, doi:10.1029/98JA00927.

Rietveld, M. T., M. J. Kosch, N. F. Blagoveshchenskaya, V. A. Kornienko, T. B. Leyser, and T. K. Yeoman (2003), Ionospheric electron heating, optical emissions, and striations induced by powerful HF radio waves at high latitudes: Aspect angle dependence, *J. Geophys. Res.*, *108*(A4), 1141, doi:10.1029/2002JA009543.

Stocker, A. J., F. Honary, T. R. Robinson, T. B. Jones, and P. Stubbe (1993), Anomalous absorption during artificial modification at harmonics of the electron gyrofrequency, *J. Geophys. Res.*, *98*(A8), 13,627–13,634, doi:10.1029/93JA00878.

Stubbe, P., H. Kopka, T. B. Jones, and T. Robinson (1982), Wide band attenuation of radio waves caused by powerful HF waves: Saturation and dependence on ionospheric variability, *J. Geophys. Res.*, *87*(A3), 1551–1555, doi:10.1029/JA087iA03p01551.

Vas'kov, V. V., and A. V. Gurevich (1976), Nonlinear resonant instability of plasma in the field of an ordinary electromagnetic wave, *Sov. Phys. JETP*, *42*(1), 91–97.